

CHAPTER ONE HUNDRED ONE

LONGSHORE SEDIMENT TRANSPORT ON DEAN BEACH PROFILES

William G. McDougal,¹ A.M., ASCE
Robert T. Hudspeth,¹ M., ASCE

Abstract

Natural beaches exhibit an equilibrium profile that is planar nearshore and non-planar, concave-up offshore. The longshore current on these Dean equilibrium beaches is shown to depend on the location of the intersection between the planar and non-planar profiles and on the dimensionless mixing strength parameter if the eddy viscosity coefficient is linearly dependent on the distance offshore. The effect of the profile intersection on the longshore sediment transport rate is demonstrated for two energetics based sediment transport models; viz. the Bagnold and energetics stress models.

Nomenclature

a	local wave amplitude;
A	dimensionless coefficient for Dean profile;
b (B)	dimensional (dimensionless) horizontal distance offshore to profile intersection;
c (C_g)	wave celerity (group celerity);
C_f	dimensionless friction coefficient for bottom stress;
d (D)	dimensional (dimensionless) total water depth including wave setup/down;
g	gravitational constant;
$G_{p(np)}$	dimensionless constant for planar (non-planar) beach profile;
h (H)	dimensional (dimensionless) still water depth;
$i_{1(2)}$ ($I_{1(2)}$)	dimensional (dimensionless) sediment transport rate for Bagnold (stress) model;
$I_\nu(\cdot)$ ($K_\nu(\cdot)$)	modified Bessel function of the first (second) kind of order ν ;
k	linear wave theory wave number;
K	dimensionless longshore sediment rate coefficient;
L	wave length;
m	roots for planar beach solution;
n	linear wave theory group velocity ratio;
N	dimensionless constant for eddy viscosity;
$P_{p(np)}$	dimensionless mixing strength parameter for planar (non-planar) beach;

¹ Ocean Engineering Program, Department of Civil Engineering, Oregon State University, Corvallis, OR 97331.

\hat{A}	dimensionless transport rate coefficient;
s, S	planar beach slope;
s_{xy}	radiation stress;
T	wave period;
u_o	magnitude of linear wave theory bottom velocity;
$v(V)$	dimensional (dimensionless) longshore current;
x, y, z	Cartesian coordinate system with z positive up from the still water level;
x_o	horizontal distance offshore to origin of concave-up profile;
ζ	dimensionless argument;
η	water surface elevation;
θ	local wave angle of incidence;
κ	dimensionless wave height to water depth ratio;
μ_e	dimensionless eddy viscosity coefficient;
π	constant;
ρ	fluid mass density; and
τ_{by}	bottom shear stress.

Introduction

Analytical solutions for longshore currents have been obtained using the concepts of radiation stresses developed for planar beaches (Bowen, 1969; Thornton, 1970; Longuet-Higgins, 1970a,b) and for non-planar, concave-up beaches (McDougal and Hudspeth, 1983a,b). In the nearshore zone inside the breaker line, the non-planar, concave-up type of beach profile seems to be generally more applicable to storm or to other high wave energy conditions. However, Dean's analysis (1977) of a total of 502 different non-storm beach profiles along the Atlantic and Gulf coasts of the United States seems to support Bruun's earlier postulation (1954, 1962) that beach profiles are typically non-planar, concave-up and vary as the horizontal distance offshore raised to the two-thirds power. Unfortunately, the Bruun type of non-planar, concave-up beach profile exhibits a mathematical singularity in the beach slope at the origin which is usually located in the swash zone. Evidently, the offshore bathymetry analyzed by Dean (1977) did not contain enough bathymetric data sufficiently close inshore to this swash zone to better resolve this concern for the mathematical singularity in the beach slope for a concave-up profile. In contrast, the nearshore observations of Komar (p.c.) seem to support the theory that non-storm beach profiles do not exhibit a singularity in beach slope near the swash zone and are often planar for the nearshore portion of the surf zone. One possible resolution of these two apparently conflicting observations is that typical non-storm beach profiles are planar nearshore and non-planar, concave-up offshore. Dean (p.c.) has recently derived a physical explanation for a planar nearshore profile. This type of composite beach profile that is planar nearshore and non-planar, concave-up offshore is probably more realistic of the actual type of beach profiles that exist during non-storm conditions and will be called a Dean beach profile.

An analysis is presented for a Dean beach profile that is planar nearshore and non-planar, $x^{2/3}$ concave-up offshore. The analysis utilizes the radiation stress concepts and incorporates an integrated, turbulent Reynolds stress tensor that is approximated by an eddy viscosity model. Although there has been some concern expressed about the justification for the various mathematical forms used to represent the turbulent eddy viscosity coefficient in the dynamic equations of motion (Battjes, 1975), the analysis by McDougal and Hudspeth (1984) of seven different mathematical expressions for the turbulent eddy viscosity coefficients demonstrated that numerical results are relatively insensitive to the exact form of the mathematical model used for non-planar, concave-up beach profiles. For this analysis, the mixing length scale of the turbulent eddy viscosity coefficient is assumed to vary linearly (Longuet-Higgins, 1970a) with the total water depth (i.e., still water depth plus wave setup/setdown). This assumed mathematical form for the mixing length scale of the turbulent eddy viscosity coefficient results in a relatively more tractable analytical model for both the planar (Longuet-Higgins, 1970a) and for the non-planar, $x^{2/3}$ concave-up Dean beach profiles (McDougal and Hudspeth, 1983a). The effects of the location of the intersection between the planar nearshore profile and the non-planar, concave-up offshore profile (i.e., $x = b$) is examined in some detail by varying the location of this intersection between the two profiles. Specifically, the profile intersection is located inside, at, and outside of the breaker line. Both the Bagnold and an energetics stress model for the longshore sediment transport (McDougal and Hudspeth, 1983b) are used to demonstrate the effects of the location of the profile intersection on the longshore sediment transport rates.

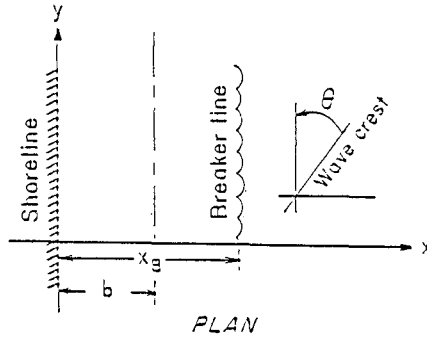
Dean Beach Profile

Figure 1 illustrates a Dean beach profile that is planar nearshore and non-planar, concave-up offshore. The horizontal distance to the intersection between the planar and non-planar profiles is located at $x = b$. Although the intersection between the planar nearshore profile and the non-planar, concave-up offshore profile is shown in Fig. 1 to be located inside the breaker line ($x = b < x_B$), it may also, in general, be located either at ($x = b = x_B$) or outside of the breaker line ($x = b > x_B$). The still water depth, $h(x)$, for the composite beach shown in Fig. 1 is given by

$$h(x) = \begin{cases} s_h x & ; x < b & (1a) \\ \alpha_h (x-x_0)^{2/3} & ; x > b & (1b) \end{cases}$$

where s_h is the planar bottom slope; α_h is a dimensional coefficient of proportionality having dimensions of length raised to the one-third power; and x_0 is the location at the still water level of the origin of the non-planar profile. The horizontal distance offshore to the origin of the non-planar profile, x_0 , and to the

Fig. 1 Definition sketch for Dean profile.



intersection between the planar and non-planar profile, b , may be related to the planar slope, s_h , and the dimensional coefficient of proportionality, α_h , by requiring continuity of depth, $h(b)$, and of profile slope, $dh(b)/dx$, at $x = b$, i.e.,

$$b^3 \zeta^3 = (b-x_0)^2 \quad (2a)$$

$$9 (b-x_0) \zeta^3 = 4 \quad (2b)$$

where

$$\zeta = (s_h / \alpha_h) \quad (2c)$$

which gives

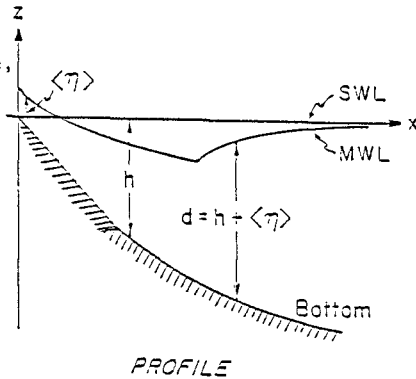
$$b = 4/9 \zeta^3 \quad (3a)$$

$$x_0 = 4/27 \zeta^3 = 1/3b \quad (3b)$$

McDougal and Hudspeth (1983a) have shown that the wave-induced setup/setdown, $\langle \eta(x) \rangle$, profiles are given by

$$\langle \eta(x) \rangle = \begin{cases} \frac{3\kappa^2}{(8+3\kappa^2)} [h_B - h(x)] - \frac{\kappa^2 h_B^2}{16} & ; x < x_B \end{cases} \quad (4a)$$

$$\langle \eta(x) \rangle = \begin{cases} -\frac{a(x)ka(x)}{2\sinh 2kh(x)} & ; x > x_B \end{cases} \quad (4b)$$



where $\langle \cdot \rangle$ = time averaging operator; $a(x)$ is the local wave amplitude; $\kappa = 2a(x)/[h(x) + \langle \eta(x) \rangle]$ is the constant of proportionality inside the breaker line between the local wave amplitude, $a(x)$, and the total water depth, $d(x) = h(x) + \langle \eta(x) \rangle$; and the local radian wave number, $k = 2\pi/L$, is determined from linear wave theory according to

$$(2\pi/T)^2 = gk \tanh kh \quad (5)$$

where T = the wave period and L = the wave length. In addition, it can be shown that the total water depth, $d(x)$, for the non-planar Bruun $x^{2/3}$ profile may be modeled in a best least-squares sense by a total water depth profile that is proportional to the horizontal distance offshore raised to the one/half power with a partial correlation coefficient of 0.986 for $0 < x < x_B$. Consequently, the total local depth profiles [i.e., still-water-depth, $h(x)$, plus setup $\langle \eta(x) \rangle$] for both the planar nearshore and the non-planar offshore profiles will be represented by

$$d(x) = \begin{cases} s_d x & ; x < b \\ \alpha_d (x - x_o)^{1/2} & ; x > b \end{cases} \quad (6a)$$

$$(6b)$$

where s_d is the slope of the total water depth. Again, continuity of the two profiles and of the two profile slopes at the location of the profile intersection, b , gives

$$b = 0.5 \lambda^2 \quad (7a)$$

$$x_o = 0.25 \lambda^2 = 0.5 b \quad (7b)$$

Nondimensionalizing all length scales by the dimensional surf zone width, x_B , (dimensional variables will be denoted by lower case letters), the following dimensionless variables (denoted by upper case letters) are introduced:

$$A = \alpha_d / \sqrt{x_B} \quad (8a)$$

$$B = b/x_B \quad (8b)$$

$$D(x) = d(x)/x_B \quad (8c)$$

$$H(x) = h(x)/x_B \quad (8d)$$

$$X = x/x_B \quad (8e)$$

$$X_o = x_o/x_B \quad (8f)$$

$$S_d = b/d(b) \quad (8g)$$

which gives the dimensionless total water depth profile as

$$D(x) = \begin{cases} S_d X & ; X < B & (9a) \\ A(X-X_o)^{1/2} & ; X > B & (9b) \end{cases}$$

Equation of Motion

The dimensional longshore depth- and time-averaged equation of motion given by Liu and Mei (1974) reduces to

$$-\frac{d}{dx} s_{xy} + \tau_{by} + \frac{d}{dx} [\mu_e d \frac{d}{dx} v] = 0 \tag{10}$$

where μ_e is the turbulent eddy viscosity coefficient; τ_{by} is the longshore component of bottom stress; v is the depth- and time-averaged longshore current component; and s_{xy} is the onshore-longshore component of the radiation stress tensor given by linear wave theory as

$$s_{xy} = -0.5 \rho g a^2 n \sin \theta \cos \theta \tag{11a}$$

$$n = 0.5 (1 + 2kh/\sinh 2kh) \tag{11b}$$

where θ is the local angle of wave incidence (vide, Fig. 1).

The gradient of the onshore-longshore component of radiation stress may be approximated by

$$\frac{d}{dx} \{s_{xy}\} = \begin{cases} -\frac{5}{16} \rho g \kappa^2 \frac{\sin \theta_B}{\sqrt{d_B}} d^{1/2} \frac{d}{dx} \{d\} & ; x < x_B & (12a) \\ 0 & ; x > x_B & (12b) \end{cases}$$

where ρ is the fluid mass density; g is the gravitational constant; and θ_B is the local angle of wave incidence at the breaker line.

The bottom shear stress is approximated by

$$\tau_{by} = -\frac{C_f}{\pi} \kappa \rho \sqrt{gd} v \tag{13}$$

where C_f is an empirically determined friction coefficient of the order of 0.01. The turbulent eddy viscosity coefficient is assumed to vary linearly with the horizontal distance offshore (McDougal and Hudspeth, 1984) according to

$$\mu_e = N \rho x \sqrt{gd} \tag{14}$$

in which N = a numerical constant. Substituting Eqs. (12) - (14) into Eq. (10) yields

$$\frac{N\pi}{\kappa C_f} \frac{d}{dx} \left\{ d^{5/2} \frac{dv}{dx} \right\} - d^{1/2} v = \begin{cases} -\frac{5}{16} \frac{\kappa\pi d^{3/2}}{C_f} \sin\theta_B \left(\frac{g}{d_B}\right)^{1/2} \frac{d}{dx}\{d\} & ; x < x_B \\ 0 & ; x > x_B \end{cases} \quad \begin{matrix} (15a) \\ (15b) \end{matrix}$$

Nondimensionalizing Eqs. (15) by the following dimensionless variables

$$S_B = d_B/x_B \quad (16a)$$

$$V = v/v_B \quad (16b)$$

where the component of the planar beach longshore current at the breaker line with no mixing is given by (Longuet-Higgins, 1970a)

$$V_B = \frac{5}{16} \frac{\kappa\pi}{C_f} \sin\theta_B \sqrt{gd_B} s_B \quad (16c)$$

reduces Eqs. (15) to

$$\frac{\pi N}{\kappa C_f} \frac{d}{dx} \left\{ D^{3/2} \frac{dV}{dX} \right\} - D^{1/2} V = \begin{cases} -\Delta D^{3/2} \frac{dD}{dX} & ; X < 1 \\ 0 & ; X > 1 \end{cases} \quad \begin{matrix} (17a) \\ (17b) \end{matrix}$$

where

$$\Delta = (x_B/d_B)^2 \quad (17c)$$

Equations (17) may be further expanded for each of the two beach profiles by substituting for the total water depth, $D(X)$, using Eqs. (9).

Planar Beach Solutions. The dynamic equations of motion for the longshore current may be obtained from Eqs. (17) by substituting Eq. (9a) to obtain

$$P_P \frac{d}{dX} \left\{ X^{5/2} \frac{dV}{dX} \right\} - X^{1/2} V = \begin{cases} -G_P X^{3/2} & ; X < 1 \\ 0 & ; X > 1 \end{cases} \quad \begin{matrix} (18a) \\ (18b) \end{matrix}$$

where the nondimensional strength of lateral mixing on a planar beach is defined by

$$P_p = \frac{\pi N S_B^2}{\kappa C_f} \tag{18c}$$

and

$$G_p = \begin{cases} B \frac{1}{(2-B)} & ; B < 1 \\ 1 & ; B > 1 \end{cases} \tag{19a}$$

$$\tag{19b}$$

The solutions to Eqs. (18) are (Longuet-Higgins, 1970a)

$$V = \begin{cases} C_{11} X^{m_1} + C_{12} X^{m_2} + \xi G_p X & ; X < 1 \\ C_{21} X^{m_1} + C_{22} X^{m_2} & ; X > 1 \end{cases} \tag{20a}$$

$$\tag{20b}$$

where

$$\xi = \frac{2}{2-5P_p} \tag{20c}$$

$$m_{1,2} = -\frac{3}{4} \pm \left(\frac{9}{16} + \frac{1}{P_p} \right)^{1/2} \tag{20d}$$

provided that $P_p \neq 0.4$.

Non-planar Beach Solutions. The dynamic equations of motion for the longshore component of current may be obtained from Eqs. (17) by substituting Eq. (9b) according to

$$P_{np} \frac{d}{dx} \left\{ \chi^{5/4} \frac{dV}{d\chi} \right\} - \chi^{1/4} V = \begin{cases} -\frac{G_{np}}{2} \chi^{1/4} & ; \chi < 1 - X_0 \\ 0 & ; \chi > 1 - X_0 \end{cases} \tag{21a}$$

$$\tag{21b}$$

where $\chi = (x-x_0)$ and the nondimensional strength of lateral mixing on a non-planar beach is defined by

$$P_{np} = \frac{\pi N A^2}{\kappa C_f} \tag{21c}$$

and

$$G_{np} = \begin{cases} \frac{2}{2-B} & ; B < 1 \\ 2B & ; B > 1 \end{cases} \tag{22a}$$

$$\tag{22b}$$

p. 152) having solutions given by

$$v = \begin{cases} a_{11}\phi_1(Z) + a_{12}\phi_2(Z) + 0.5G_{np} & ; X < 1 & (23a) \\ a_{22}\phi_1(Z) & ; X > 1 & (23b) \end{cases}$$

where

$$\phi_1(Z) = Z^{-1/8} I_{1/4}(\gamma Z^{1/2}) \quad (23c)$$

$$\phi_2(Z) = Z^{-1/8} K_{1/4}(\gamma Z^{1/2}) \quad (23d)$$

$$Z = X - B/2 \quad (23e)$$

$$\gamma = \frac{2}{\sqrt{P}_{np}} \quad (23f)$$

Evaluation of the longshore component of velocity, v , on a Dean beach requires solving Eqs. (18) for the planar nearshore component when $X < B$ and Eqs. (21) for the non-planar offshore component when $X > B$. Since both Eqs. (18) and (21) are of second-order, continuity of the magnitude and the slope of the current will be required at $X = B$ in order to quantify these unknown constants of integration. In order to evaluate the effect of the location of the intersection of the planar and non-planar profiles at $X = B$, the unknown constants of integration in Eqs. (20) and (23) will be determined for each of the three separate locations; viz. 1) inside the breaker line ($B < 1$); 2) at the breaker line ($B = 1$); and 3) outside the breaker line ($B > 1$). The matching conditions to be used at the intersection of the two profiles are: 1) continuity of longshore current magnitudes

$$V_{<} = V_{>} ; X = B \quad (24a)$$

and 2) continuity of the gradient of the longshore currents

$$\frac{d}{dX} V_{<} = \frac{d}{dX} V_{>} ; X = B \quad (24b)$$

where $V_{<}$ is the current for $X < B$ and $V_{>}$ is the current for $X > B$.

B < 1 Solutions. When the profile intersection is located inside the breaker line, $B < 1$, the solutions are given by

$$v = \begin{cases} C_{11} X^m + \xi G_p X & ; X < B & (25a) \\ a_{11}\phi_1(Z) + a_{12}\phi_2(Z) + G_{np}/2 & ; B < X < 1 & (25b) \\ a_{22}\phi_2(Z) & ; X > 1 & (25c) \end{cases}$$

where Z is defined by Eq. (23e) and

$$a_{11} = G_{np} Z^{3/2} \phi_3(\zeta) \quad ; \quad \zeta = 1 - B/2 \quad (26a)$$

$$a_{12} = \frac{a_{11} [m_1 \phi_1(\zeta) - B \phi_4(\zeta)] - \xi G_p B^{(m_1-1)} + 0.5 m_1 G_{np}}{B \phi_3(\zeta) - m_1 \phi_2(\zeta)} \quad ; \quad \zeta = B/2 \quad (26b)$$

$$a_{22} = \frac{a_{11} \phi_1(\zeta) + 0.5 G_{np}}{\phi_2(\zeta)} + a_{12} \quad ; \quad \zeta = 1 - B/2 \quad (26c)$$

$$C_{11} = B^{-m_1} [a_{11} \phi_1(\zeta) + a_{12} \phi_1(\zeta) + 0.5 G_{np} - \xi G_p B] \quad ; \quad \zeta = B/2 \quad (26d)$$

$$\phi_3(\zeta) = -\frac{\zeta}{4}^{-9/8} [K_{1/4}(\gamma \zeta^{1/2}) + 2\gamma \zeta^{1/2} K_{-3/4}(\gamma \zeta^{1/2})] \quad (26e)$$

$$\phi_4(\zeta) = -\frac{\zeta}{4}^{-9/8} [I_{1/4}(\gamma \zeta^{1/2}) - 2\gamma \zeta^{1/2} I_{-3/4}(\gamma \zeta^{1/2})] \quad (26f)$$

B = 1 Solutions. When the location of the profile intersection coincides with the location of the breaker line, $B = 1$, the solutions are given by

$$v = \begin{cases} C_{11} X^{m_1} + \xi G_p X & ; X < 1 \quad (27a) \\ a_{22} \phi_2(Z) & ; X > 1 \quad (24b) \end{cases}$$

where Z is defined by Eq. (23e) and

$$a_{22} = \frac{(m_1-1) \xi G_p}{m_1 \phi_2(\zeta) - \phi_3(\zeta)} \quad ; \quad \zeta = 1 - B/2 \quad (28a)$$

$$C_{11} = a_{22} \phi_2(\zeta) - \xi G_p \quad ; \quad \zeta = 1 - B/2 \quad (28b)$$

B > 1 Solutions. When the profile intersection is located outside the breaker, $B > 1$, the solutions are given by

$$v = \begin{cases} C_{11} X^{m_1} + \xi G_p X & ; X < 1 < B \quad (29a) \\ C_{21} X^{m_1} + C_{22} X^{m_2} & ; 1 < X < B \quad (29b) \\ a_{22} \phi_2(Z) & ; X > B > 1 \quad (29c) \end{cases}$$

where Z is defined by Eq. (23e) and

$$C_{22} = \frac{(m_1 - 1) \xi G_p}{m_1 - m_2} \tag{30a}$$

$$C_{21} = \frac{C_{22} [m_2 \phi_2(\zeta) - B \phi_3(\zeta)] B^{(m_2 - m_1)}}{B \phi_3(\zeta) - m_1 \phi_2(\zeta)} \quad ; \quad \zeta = B/2 \tag{30b}$$

$$C_{11} = C_{21} + C_{22} - \xi G_p \tag{30c}$$

$$C_{22} = \frac{C_{21} B^{m_1} + C_{22} B^{m_2}}{\phi_2(\zeta)} \quad ; \quad \zeta = B/2 \tag{30d}$$

Figures 2 and 3 demonstrate the effects of the offshore distance to the profile intersection $X = B$, on the longshore current profile, V , for mixing strengths $P_p = P_{np}$ equal to 0.1 and 1.0, respectively. Two longshore current profiles are shown for $B < 1.0$ (viz. $B = 0.1$ and 0.5) and one profile each for $B = 1$ and for $B > 1$ (viz. $B = 1.95$). These profiles demonstrate that the magnitude of the longshore current profile decreases with increasing magnitude of the dimensionless mixing strength parameter P_p [cf. Eq. (18c)] for planar beaches and P_{np} [cf. Eq. (21c)] for non-planar beaches. The horizontal offshore distance, X , to the maximum longshore current decreases with decreasing values of the horizontal distance to the profile intersection, B , for $B < 1$. However, the magnitude of the maximum longshore current increases with increasing values of the horizontal distance to the profile intersection, B , for $B < 0.8$. The magnitudes then decrease with increasing values of B for $0.8 < B < 1.0$.

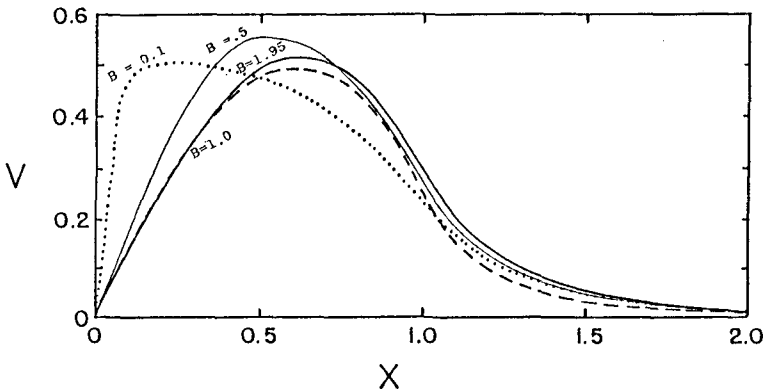


Fig. 2 Effect of profile intersection, B , on the longshore current profile, V ($P_p = P_{np} = 0.1$).

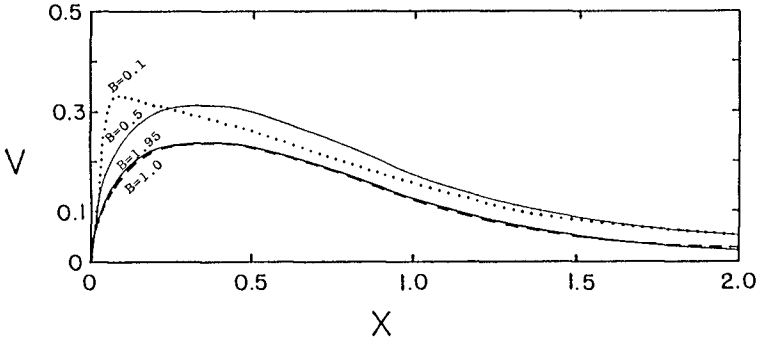


Fig. 3 Effect of profile intersection, B , on the longshore current profile, V $\{P_p = P_{np} = 1.0\}$.

Figure 4 demonstrates the effect of the location of the profile intersection, B , on the magnitude of the maximum longshore component of velocity, V_{max} , for two values of the dimensionless mixing strength parameters.

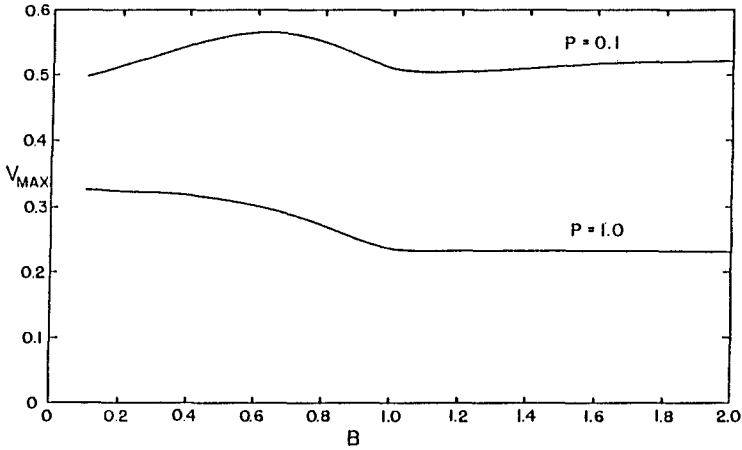


Fig. 4 Effect of profile intersection, B , on the maximum magnitude of the longshore current, V_{max} .

Energetics Sediment Transport Models

The magnitude of the longshore current is required for the evaluation of the longshore transport of sand. Since the current profiles for the Dean beach profiles differ significantly from those predicted analytically for planar beaches, the corresponding sediment transport profiles should also be expected to differ. The longshore transport profiles of sand are developed using the following two energetics-based transport models: (1) the Bagnold-type model (Bagnold, 1963) which has been widely used in surf zone applications (cf. Inman and Bagnold, 1963; Komar and Inman, 1970; Komar, 1971, 1975, 1977; Thornton, 1973; Bowen, 1978; Walton and Chiu, 1979); and (2) an energy-dissipation model based on the total stress exerted on the sand by the mean wave-induced current (cf. Komar, 1971; Bailard and Inman, 1981; McDougal and Hudspeth, 1983b). The energetics stress model has been calibrated with the Bagnold model for a planar beach in which the dimensionless transport rate coefficient, K , for the Bagnold model has previously been evaluated by Komar (1975).

Bagnold Model

Bagnold (1963) proposed a sand transport model which includes both bed load and suspended load. This model assumes that the orbital wave motion mobilizes the beach sand and wave power is then expended maintaining the sand in motion. The presence of a mean current, regardless of how small, transports the sand. The Bagnold immersed-weight transport rate per unit width of surf zone, i_1 , for small angles of wave incidence is (cf. Thornton, 1973):

$$i_1 = K \frac{d}{dx} \left(\frac{1}{2} \rho g a^2 c_g \right) \frac{v}{u_o} \quad (31)$$

in which K is a dimensionless transport rate coefficient; a is the local wave amplitude; c_g is the wave group velocity; and u_o is the magnitude of the near-bottom orbital wave velocity. Assuming that shallow-water, linear wave conditions exist ($c_g = \sqrt{gd}$) and that the local wave amplitude is proportional to the total water depth, d , (i.e., $2a = \kappa d$), the immersed transport rate in the longshore direction shoreward of the breaker line reduces to:

$$i_1 = \frac{5}{8} K \rho g \kappa d v \frac{d}{dx} d \quad ; x < x_B \quad (32)$$

Nondimensionalizing the longshore transport rate by the breaker line sand transport on a planar beach due to the no-mixing longshore current (cf. Longuet-Higgins, 1970a), i_{BL1} , the dimensionless longshore transport profile is given by:

$$I_1 = \frac{i_1}{i_{BL1}} = \begin{cases} v \frac{D}{D_B} \frac{d}{dX} \left(\frac{D}{D_B} \right) & ; X < 1 & (33a) \\ 0 & ; X > 1 & (33b) \end{cases}$$

in which

$$i_{BL1} = \frac{5}{2} K \frac{\rho g}{\kappa} \frac{a_B^2}{x_B} v_{LH} \tag{33c}$$

$$v = v/v_{LH1} = v/\frac{5}{16} \frac{\pi \kappa}{C_f} s_d \sqrt{gd_B} \sin \theta_B \tag{33d}$$

where π is a numerical constant and C_f is a dimensionless friction coefficient of order 0.01.

For a planar beach, the Bagnold model sediment transport profile is given by

$$I_1 = \begin{cases} XV & ; X < 1 & (34a) \\ 0 & ; X > 1 & (34b) \end{cases}$$

For a concave-up $x^{1/2}$ beach profile, the Bagnold sediment transport model becomes

$$I_1 = \begin{cases} \frac{1}{2} V & ; X < 1 & (35a) \\ 0 & ; X > 1 & (35b) \end{cases}$$

Figure 5 demonstrates the effect of the dimensionless profile intersection, B , as the longshore sediment transport rates, I_1 , computed by the Bagnold model for two extreme values of the dimensionless mixing strength parameter $\{P_p = P_{np} = 0.1 \text{ and } 1.0\}$.

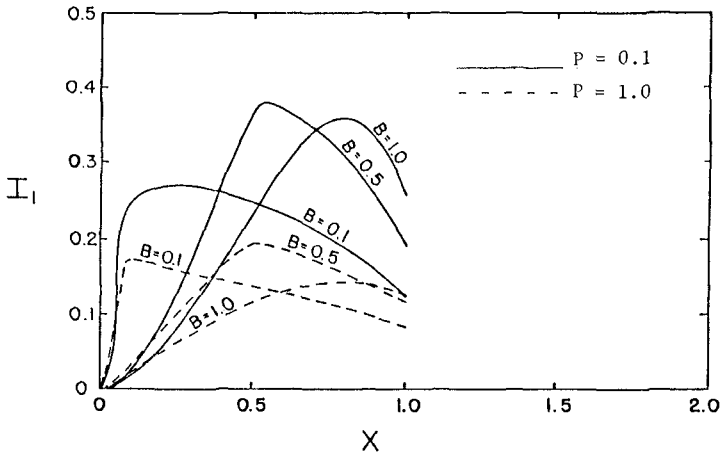


Fig. 5 Effect of profile intersection, B , on Bagnold longshore sediment transport rates, I_1 .

Stress Model

Komar (1971) proposed a swash sediment transport model based on the energy dissipation associated with the bottom stress. Bailard and Inman (1981) also developed an energetics stress model using the bottom stress to estimate the time-dependent bedload transport in the surf zone. These models are both Bagnold-type models conceptually; but since the energy dissipation rate or available power for mobilizing sediment is based on the bottom stress, these models are termed stress models. The immersed-weight transport rate per unit width of surf zone, i_2 , for the stress model for small angles of incidence is (cf. McDougal and Hudspeth, 1983a)

$$i_2 = c_5 \rho |u_o| v^2 \sin\theta \quad (36a)$$

in which c_5 is a constant for a given sediment and

$$u_o = a \frac{k}{\omega} \operatorname{sech}(kd) (\hat{i} + \sin\theta \hat{j}) \quad (36b)$$

in which ω = the radian wave frequency.

Note that in Eq. (36a), no shallow-water wave assumptions have been invoked and no restrictions have been placed on the mechanism which generates the longshore current. This model may be used for high wind- or tide-induced flows as well as for wave-induced long-shore currents.

As in Eqs. (33), the transport rate is nondimensionalized by the transport rate at the breaker line from a stress model on a plane beach using the no-mixing velocity determined by Longuet-Higgins (1970a). The dimensionless transport, I_2 , is given by

$$I_2 = \frac{\sin\theta}{\sin\theta_B} \frac{u_o}{u_{oB}} v^2 \quad (37a)$$

in which

$$I_2 = i_2/i_{BL2} = i_2 / (c_5 \rho |u_{oB}| v_{LH}^2 \sin\theta_B) \quad (37b)$$

Employing Snell's law for refraction, the transport rate reduces to

$$I_2 = \frac{a}{a_B} v^2 \quad (38)$$

in which the hyperbolic cosines have been approximated by unity in the surf zone. This transport relationship applies for any type of beach profile and mean current.

Komar (1975) has determined the transport coefficient for the Bagnold model on a planar beach by comparison with observed total transports. The total transport is defined by

$$I_T = \int_0^{\infty} I \, dX \quad (39)$$

The stress model is calibrated by equating the total transport on a planar beach with that for the calibrated Bagnold model. This yields a dimensionless transport coefficient for the stress model, R ,

which is a function of the lateral turbulent mixing strength parameter, P_p .

Figure 6 demonstrates the dependence of the dimensionless transport rate coefficient on the dimensionless mixing strength parameter.

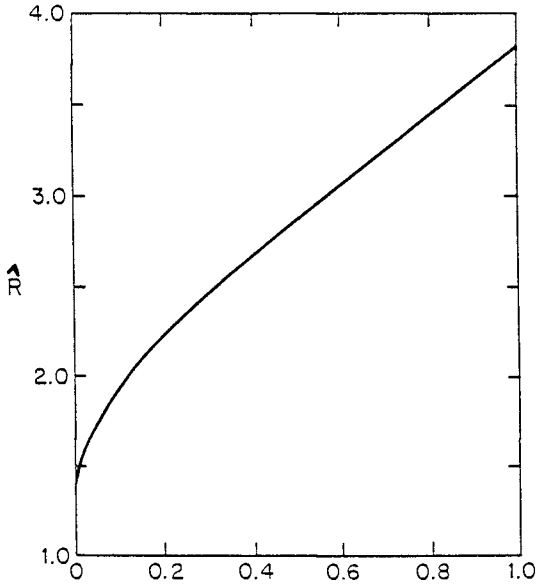


Fig. 6 Dimensionless stress transport rate coefficient calibrated with a Bagnold transport rate for a planar beach.

The longshore transport rate given by the stress model for a planar beach (including the calibration coefficient) is

$$I_2 = \begin{cases} \hat{R} X V^2 & ; X < 1 & (40a) \\ \hat{R} V^2 & ; X > 1 & (40b) \end{cases}$$

The longshore transport rate given by the stress model for a concave-up beach is

$$I_2 = \begin{cases} \hat{R} X^{1/2} V^2 & ; X < 1 & (41a) \\ \hat{R} V^2 & ; X > 1 & (41b) \end{cases}$$

Figure 7 demonstrates the effect of dimensionless profile intersection, B , on the longshore sediment transport rates, I_2 , computed by a stress model for two extreme values of the dimensionless mixing strength parameters.

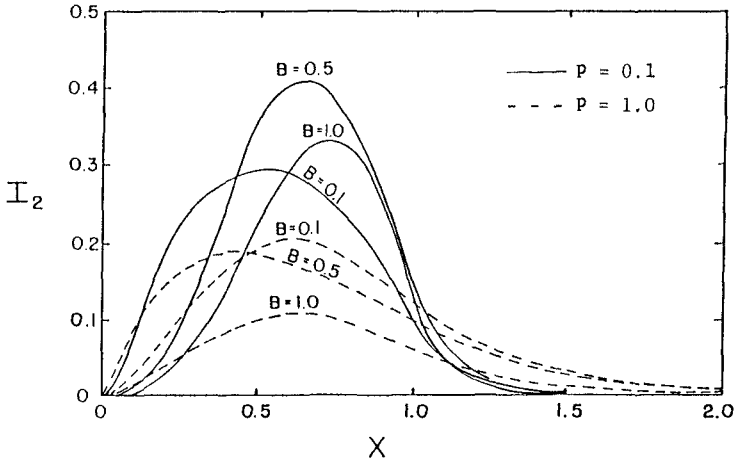


Fig. 7 Effect of profile intersection, B , on stress-type longshore sediment transport rates, I_2 .

Conclusions

Dimensionless longshore current profiles, V , on equilibrium Dean beach profiles depend on both the location of the dimensionless horizontal distance offshore to the profile intersection, B , and the dimensionless mixing strength parameters, P_n and P_{np} . The maximum dimensionless longshore current, V_{max} , occurs near a value of $B = 0.8$. The dimensionless longshore current profiles, V , are essentially independent of B for $B > 1$. The longshore current, V , decreases with increasing values of dimensionless mixing strength, P . The effect of the dimensionless profile intersection, B , and mixing strength parameter, P , is similar for both Bagnold and stress type longshore sediment transport rates.

Acknowledgements

This research was supported by the Oregon State University Sea Grant College Program, National Oceanic and Atmospheric Administration Office of Sea Grant, Department of Commerce, under Grant No. NA81AA-D-00-086 (Project NO. R/CE-13). The U.S. government is authorized to produce and distribute reprints for governmental purposes, notwithstanding any copyright notation that may appear hereon.

References

1. Bagnold, R.A., 1963. Beach and nearshore processes, Part I. In: Mechanics of Marine Sedimentation. The Sea, M.N. Hill (Editor), pp. 507-528.
2. Bailard, J.A. and Inman, D.L., 1981. An energetics bedload model for a plane sloping beach: Local transport. J. Geophys. Res., 86, pp. 2035-2043.
3. Battjes, J.A., 1975. Modeling of turbulence in the surf zone. Proc. Symp. Modeling Techniques, pp. 1050-1061.
4. Bowen, A.J., 1969. The generation of longshore currents on a plane beach. J. Mar. Res., 27, pp. 206-214.
5. Bowen, A.J., 1978. Simple models of nearshore sedimentation, beach profiles and longshore bars. Proc. Conf. Coastlines of Canada.
6. Bruun, P., 1954. Coast Erosion and Development of Beach Profiles. Beach Erosion Board, Tech. Memo. No. 44, 82 pp.
7. Bruun, P., 1962. Sea-level rise as a cause of shore erosion. J. Waterways Harbors Div., Am. Soc. Civ. Engrs., 88, pp. 117-130.
8. Dean, R.G., 1977. Equilibrium Beach Profiles: U.S. Atlantic and Gulf Coasts, Univ. of Delaware, Ocean Engineering Report No. 12, 45 pp.
9. Hildebrand, F.B., 1976. Advanced Calculus for Applications (Second Edition), Prentice-Hall, Englewood Cliffs, NJ, p. 152.
10. Inman, D.L. and Bagnold, R.A., 1963. Beach and nearshore processes. Part II. Littoral processes. In: The Sea, M.N. Hill (Editor), pp. 529-553.
11. Komar, P.D., 1971. The mechanics of sand transport on beaches. J. Geophys. Res., 76, pp. 713-721.
12. Komar, P.D., 1975. Longshore currents and sand transports on beaches. Proc. Civil Eng. in the Oceans/III, 1, pp. 333-354.
13. Komar, P.D., 1977. Beach sand transport: Distribution and total drift. J. Waterway, Port, Coast Ocean Div., Am. Soc. Civ. Eng., 103, pp. 225-239.
14. Komar, P.D. and Inman, D.L., 1970. Longshore sand transport on beaches. J. Geophys. Res., 75, pp. 5914-5927.
15. Liu, P.L.-F. and Mei, C.C., 1974. Effects of a Breakwater on Nearshore Currents due to Breaking Waves. Ralph M. Parson Laboratory, Department of Civil Engr., Massachusetts Inst. of Tech., Report No. 12, 243 pp.
16. Longuet-Higgins, M.S., 1970a. Longshore currents generated by obliquely incident sea waves, 1. J. Geophys. Res., 75, pp. 6778-6789.
17. Longuet-Higgins, M.S., 1970b. Longshore currents generated by obliquely incident sea waves, 2. J. Geophys. Res., 75, pp. 6790-6801.
18. McDougal, W.G. and Hudspeth, R.T., 1983a. Wave setup/setdown and longshore current on non-planar beaches. Coastal Eng., 7, pp. 103-117.

19. McDougal, W.G. and Hudspeth, R.T., 1983b. Longshore Sediment Transport on Non-Planar Beaches. Coastal Eng., 7, pp. 119-131.
20. McDougal, W.G. and Hudspeth, R.T., 1984. Comparison of turbulent lateral mixing models. J. Mar. Res. (in review).
21. Thornton, E.B., 1970. Variation of longshore current across the surf zone. Proc. 12th Coastal Engrg. Conf., ASCE 291-308.
22. Thornton, E.B., 1973. Distribution of sediment transport across the surf zone. Proc. 13th Conf. Coastal Eng., pp. 1049-1068.
23. Walton, T.L. and Chiu, T.Y., 1979. A review of analytical techniques to solve the sand transport equation and some simplified solutions. Proc. Spec. Conf. Coastal Structures, pp. 809-837.